Journal of Orthopaedics and Physiotherapy
Volume 4 | Issue 1
ISSN: 2639-930X

Research Article Open Access

Rotational Effect on Waves Propagation Modeling in a Poroelastic Bone

Abd-Alla AM[*1], Abo-Dahab SM[2,3], Abdelhafez MA[1] and El-Teary H[1]

[1]Mathematics Department, Faculty of Science, Sohag University, Sohag, Egypt

[2]Mathematics Department, Faculty of Science, South Valley University, Egypt

[3]Department of Computer Science, Faculty of Computers and Information, Luxor University, Egypt

[*]**Corresponding author:** Abd-Alla AM, Mathematics Department, Faculty of Science, Sohag University, Sohag, Egypt, Tel: +201121866266, E-mail: mohmrr@yahoo.com

Citation: Abd-Alla AM, Abo-Dahab SM, Abdelhafez MA, El-Teary H (2021) Rotational Effect on Waves Propagation Modeling in a Poroelastic Bone. J Orthop Physiother 4(1): 103

Received Date: April 20, 2021 **Accepted Date:** June 01, 2021 **Published Date:** June 03, 2021

Abstract

In this work, the dynamic behavior of a wet long bone that has been modeled as transversely isotropic hollow cylinder of crystal class 6 subjected to rotation is investigated. The solution wave for the wave propagation problem is expressed in term of a potential function which satisfies an eight-order partial differential equation, whose solutions lead to the derivation of the explicit solution of the wave equation. The mechanical boundary conditions corresponds to those of stress free lateral surface, while the fluid boundary condition correspond to of fluid stress free lateral surfaces. The satisfaction of the boundary conditions leads to the dispersion relation which is solved numerically. These frequencies are computed for poroelastic bone in terms of several values of the rotation and bone porosity.The results can benefit the theoretical development of orthopedic study projects connected to cylindrical poroelastic long bones. A comparison was made between the theoretical findings and the in vitro experimental values reported by a previously developed non-contacting device.

Keywords: Poroelastic Medium; Rotation; Wave Propagation; Wet Bone; Porous Media; Natural

Introduction

The tissues of the bones are categorized into two types. The first type is the cancellous bone whose volume fraction of solid is low (less than 70%), whereas the second type is known as the cortical bone that has more than 70% solid field. Cancellous bone consists of two components, namely fatty marrow in the pores and calcified bone matrix. The study of the propagation of waves over a continuous medium is important practically in bio-engineering, medicine, and engineering. Moreover, applying poroelastic materials in some fields of medicine, e.g., orthopedics, dentistry, and cardiovascular medicine are common. In orthopedics, the propagation of waves through bone shelpsmonitor the rate of fracture curing. Theoretical wave propagation problems in wet bone are also considered [1-4]. Biot [5] developed the fundamental relation and consolidation for poroelastic media. The authors of [6] explored the stresses in human long bones. A micro-level 3D computational study of Wolff's law via the remodeling of trabecular bone in the human proximal femur using design space topology optimization was investigated by Boyle and Kim [7]. Elastic wave propagation for the surface bone of alveolar bone remodeling was studied by Mengoni and Ponthot [8]. Internal remodeling of poroelastic bone was investigated by Papathanasopoulou et al. [9]. The surface of the remodeling of bone under electromagnetic loads was studied by Qu et al. [10]. The surface waves of the remodeling of bone show several dynamic responses in disuse and overload,as studied by Hazelwood et al. [11]. Additionally, the authors of [12] examined the mechanical adaptation of trabecular bone combining cellular accommodation and the impacts of micro damage and disuse. Thenumerical calculations of the remodeling of bones sensitive to harmonic load over a poroelastic performance were studied by Malachanne et al. [13]. General analysis of mathematical models of the remodeling of bones was investigated by Zumsande et al. [14]. Ramtani and He [15] investigated the surface of wet of the remodeling of bone driven by metallic pin fitted into the medulla of a long bone. Ganghoffer [20] studied the surface growth's mechanics and thermodynamics. The authors of [16] explored the surface of the remodeling of bones of diaphysial surfaces under frequency load. Tsili [27] obtained the phase velocity for the internal remodeling of bones of diaphyseal shafts using Lame's potential.Jang and Kim [18] discussed the numerical simulations of simultaneous cortical and trabecular bone changesin the human proximal femur during the remodeling of bones. Martínez et al. [19] examined the propagation of waves in wet bone in damage mechanics and boundary elements. The authors of [20] solved analytically the thermo-electro-elastic for the remodeling of surface bones subjected to axial and transverse loads. Kameo et al. [21] explored the functional adaptation of trabeculae predicted by the remodeling of bones subjected to loading frequency. The dynamic behavior method such as wave propagation and vibration of bone is necessary in measuring in vivo properties of bone by the above non-invasive method [22-29].

In the present paper, we explore the propagation of waves in poroelastic bone subjected to a rotation. The analytical solution for the propagation of waves in a wet bone subjected to a rotation was obtained, which satisfies the fundamental equation whose solutions lead to the derivation of the frequency equations for certain boundary circumstances. The numerical solution of the equations of frequency was obtained using the bisection method.The numerical findings showed the applicability of the proposed solutions and the impact of the rotation on the surface of the bones. The coefficients of the poroelastic bone were concluded for the different values of the rotation and the porosity of bones.

Formulation of the problem

The system of solid plus fluid is assumed to be a system with conservation properties. The solid part is considered to have compressibility and shearing rigidity and the fluid to be compressible. The deformation of a unit cube is assumed is assumed to be completely reversible. The system geometry is defined by providing cylindrical coordinates $r, \theta, z,$ as shown in Figure 1.

Modelling on the concept of the Biot [5] the constitutive equations for a transversely isotropic case with z as the axis of the symmetry are taken in polar coordinates as

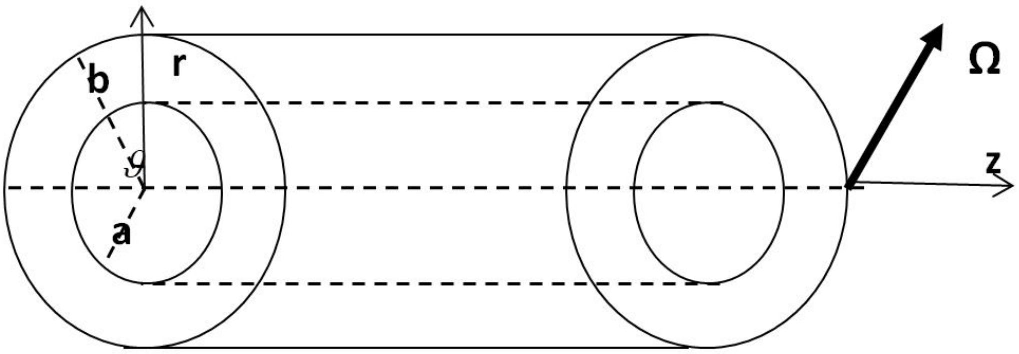

Figure 1: Schematic of the problem

$$\sigma_{rr} = c_{11}u_{r,r} + c_{12}r^{-1}(u_r + u_{\theta,\theta}) + c_{13}u_{z,z} + M[v_{r,r} + r^{-1}(v_r + v_{\theta,\theta}) + v_{z,z}]$$

$$\sigma_{\theta\theta} = c_{12}u_{r,r} + c_{11}r^{-1}(u_r + u_{\theta,\theta}) + c_{13}u_{z,z} + M[v_{r,r} + r^{-1}(v_r + v_{\theta,\theta}) + v_{z,z}] \quad (1)$$

$$\sigma_{zz} = c_{13}[u_{r,r} + r^{-1}(u_r + u_{\theta,\theta})] + c_{33}u_{z,z} + Q[v_{r,r} + r^{-1}(v_r + v_{\theta,\theta}) + v_{z,z}]$$

$$\sigma_{\theta z} = c_{44}[u_{\theta,z} + r^{-1}u_{z,\theta}]$$

$$\sigma_{rz} = c_{44}[u_{r,z} + u_{z,r}]$$

$$\sigma_{r\theta} = c_{66}[u_{\theta,r} + r^{-1}(u_{r,\theta} - u_\theta)]$$

$$\sigma = M[u_{r,r} + r^{-1}(u_{\theta,\theta} - u_r)] + Qu_{z,z} + R[v_{r,r} + r^{-1}(v_r + v_{\theta,\theta}) + v_{z,z}]$$

The σ_{ij} (i,j=1,2,3) and σ are the average stresses of solid and fluid, respectively , with elastic constants C_{ij}, *M, Q, R* and $c_{66} = (c_{11} - c_{12})/2$

The equation of motion of the flow is

$$\frac{1}{b_{rr}}\nabla^2\sigma + \frac{1}{b_{zz}}\sigma_{zz} = (\varepsilon - \sigma)_{,t} \quad (2)$$

where $b_{rr} = \dfrac{\mu f^2}{k_{rr}}$, $b_{zz} = \dfrac{\mu f^2}{k_{zz}}$ *and* $\nabla^2 = \dfrac{\partial^2}{\partial r^2} + \dfrac{1}{r}\dfrac{\partial}{\partial r} + \dfrac{\partial^2}{\partial\theta^2}$ is a Laplacian operator in polar coordinates, μ is the viscosity, *f is* the porosity and k_{rr}, k_{zz} are the permeability of the medium. The average displacements of solid and velocity of fluid phases are taken as u_i and v_i respectively.The strains are expressed as

$$e_{ij} = \frac{u_{i,j} + u_{j,i}}{2} \quad (3)$$

and dilation of the phases as $e = u_{i,i}$ and $\varepsilon = v_{i,i}$

For a material of crystal class 6 the equations of motion in cylindrical coordinates are given as

$$\sigma_{rr,r} + r^{-1}\sigma_{r\theta,\theta} + \sigma_{rz,z} + r^{-1}(\sigma_{rr} - \sigma_{\theta\theta}) = \rho[u_{r,tt} - \Omega^2 u_r + 2\Omega u_{z,t}$$

$$\sigma_{\theta z,z} + r^{-1}\sigma_{\theta\theta,\theta} + \sigma_{r\theta,r} + 2r^{-1}\sigma_{r\theta} = \rho u_{\theta,tt} \quad (4)$$

$$\sigma_{rz,r} + r^{-1}\sigma_{rz} + r^{-1}\sigma_{\theta z,\theta} + \sigma_{zz,z} = \rho[u_{z,tt} - \Omega^2 u_z + 2\Omega u_{r,t}]$$

Solution of the problem

Consider a homogeneous, transversely isotropic, infinite hollow poroelastic cylinder with inner and outer radii *a* and *b* respectively, having a thickness *h* whose axis is in the direction of the *z*-axis.

Let

$$\begin{aligned} u_r &= [\varphi_{,r} + r^{-1}\psi_{,\theta}]\exp i(kz - pt) & u_\theta &= [r^{-1}\varphi_{,\theta} - \psi_{,r}]\exp i(kz - pt) \\ u_z &= [iw/h]\exp i(kz - pt) & v_r &= -\eta_r \exp i(kz - pt) \\ v_\theta &= -\eta_{,\theta} \exp i(kz - pt) & v_z &= -ik\eta \exp i(kz - pt) \end{aligned} \quad (5)$$

where $u_r, u_\theta, u_z, v_r, v_\theta, v_z$ are mechanical displacements and velocities, k is the wavenumber, p is the frequency and h is the thickness of the cylinder $h = b - a$, Ω is the rotation and ϕ, ψ, w, η are secular potentials and it functions of r and θ.

Substituting (1),(3),into the equations(2),(4),and using (5), the following equations are obtained.

$$(c_{11}\nabla^2 + \rho p^2 + \rho\Omega^2 - k^2 c_{44})\varphi - ((c_{44} + c_{13})k + 2i\Omega p\rho)\frac{w}{h} - M(\nabla^2 - k^2)\eta = 0$$

$$(c_{66}\nabla^2 - c_{44}k^2 + \rho p^2 - \rho\Omega^2)\psi = 0$$

$$((c_{44} + c_{13})k\nabla^2 - 2\rho p\Omega)\varphi + (c_{44}\nabla^2 + \rho p^2 + \rho\Omega^2 - c_{33}k^2)\frac{w}{h} + KQ(\nabla^2 - k^2)\eta = 0 \quad (6)$$

$$(\frac{\nabla^4}{b_{rr}} - k^2\frac{\nabla^2}{b_{zz}} - ip\nabla^2)M\varphi + (-\frac{\nabla^2}{b_{rr}} + \frac{k^2}{b_{zz}} + \frac{ip}{h})kQ\frac{w}{h} + (-\frac{\nabla^2}{b_{rr}} + \frac{k^2}{b_{zz}} + ip)(\nabla^2 - k^2)R\eta = 0$$

By defining the dimensionless, coordinate $x = \frac{r}{h}$ and $\varepsilon = kh$ the above equations are written in dimensionless parameter *x* and ε as

$$(c'_{11}\nabla^2 + (ch)^2 + (ch\Omega')^2 - \varepsilon^2)\phi - ((1 + c'_{13})\varepsilon + 2i\Omega' c^2 h)w - M'\eta = 0$$

$$[(1 + c'_{13})\nabla^2\varepsilon - 2\Omega' c^2 h^3]\phi + [\nabla^2 + (ch)^2 + (ch\Omega')^2 - c'_{33}\varepsilon^2]w + Q'\varepsilon\eta = 0$$

$$\begin{aligned} &\nabla^2[\nabla^2 M' - \varepsilon^2 bM' - iM'^2 c_{44} D]\phi + [-\nabla^2 Q' + \varepsilon^2 bQ' + \frac{iM' c_{44} DQ'}{h}]\varepsilon w + \\ &+ [-\nabla^2 R'M' + \varepsilon^2 bR'M' + iM'^2 c_{44} R'D]\eta = 0 \end{aligned} \quad (7)$$

$$[c'_{66}\nabla^2 - \varepsilon^2 + (ch)^2 - (ch\Omega')^2]\psi = 0 \tag{7a}$$

where

$$D = \frac{ph^2 b_{rr}}{M},\ Q' = \frac{Q}{M},\ R' = \frac{R}{M},\ b = \frac{b_{rr}}{b_{zz}},\ M' = \frac{M}{c_{44}},\ Q' = \frac{Q}{c_{44}},\ and\ \xi = (\nabla^2 - \varepsilon^2)\eta$$

The reason for ξ being defined as above and not been solved for the variation is that the flow of fluid through the boundaries of bone does not take place during the study of the propagation of waves. However can be calculated if the flow of the boundaries is prescribed.

Writing an equation (7) in the determinants from

$$\begin{vmatrix} c'_{11}\nabla^2 + A + (ch\Omega')^2 & -(B + 2ic^2h\Omega') & -M' \\ B\nabla^2 - 2c^2h^3 & \nabla^2 + C + (ch\Omega') & \varepsilon Q' \\ B1 & B2 & B3 \end{vmatrix}(\varphi, w, \eta) = 0 \tag{9}$$

where

$$B1 = \nabla^2[\nabla^2 M' - \varepsilon^2 bM' - iDM'^2 c_{44}],\ B2 = (-\nabla^2 + C + (ch\Omega')^2)\varepsilon Q'\ ,$$

Evaluating the determinant form, the following equations are obtained

$$B3 = -\nabla^2 R'M' + \varepsilon^2 bR'M' + iR'M'^2 Dc_{44},\ A = (ch)^2 - \varepsilon^2, B = (1 + c'_{13})\varepsilon\ and\ C = (ch)^2 - c'_{33}\varepsilon^2$$

$$(\nabla^6 + S\nabla^4 + U\nabla^2 + H)(\phi, w, \eta) = 0 \tag{10}$$

$$S = [-AR'M' - R'M'(ch\Omega')^2 + R'M'B^2 - BQ'R'M'\varepsilon - 2i\Omega'c^2hB - 2iQ'M'\varepsilon c^2h + B\varepsilon Q'M' - \varepsilon^2 b - iDc_{44} + C + (ch\Omega')^2 - Q'^2\varepsilon^2 R'M'] / (M'^2 - c'_{11}R'M')$$

$$\begin{aligned} U = [&-C\varepsilon^2 b - iCDc_{44} - \varepsilon^2 b(ch\Omega')^2 - iD(ch\Omega')^2 c_{44} - c'_{11}Q'^2\varepsilon^4 b - iDc'_{11}\nabla^2 Q'^2\varepsilon^2 c_{44}M' + A\varepsilon^2 bR'M' + \\ &iDAc_{44}R'M' - ACR'M' - AR'M'(ch\Omega')^2 + AQ'^2\varepsilon^2 + (ch\Omega')^2\varepsilon^2 bR'M' + iD(ch\Omega')^2 c_{44}R'M' - (ch\Omega')^2 CR'M' - \\ &(ch\Omega')^4 R'M' + (ch\Omega')^2 Q'^2\varepsilon^2 + B^2\varepsilon^2 bR'M' + iDB^2 c_{44}R'M' + 2B\Omega'c^2h^3R'M' + BQ'\varepsilon^2 bM' + iBQ'\varepsilon M'c_{44} + \\ &2i\Omega'c^2hB\varepsilon^2 bR'M' - 2\Omega'c^2hBDc_{44}R'M' + 4i\Omega'^2c^4h^4R'M' + 2i\Omega'c^2hQ'\varepsilon^2 bM' - 2c^2h\Omega'Q'\varepsilon DM'c_{44} - \\ &B\varepsilon^2 bQ'M' - iDBQ'\varepsilon M'^2 c_{44} / h - 2\Omega'c^2h^3\varepsilon Q'M'] / (M'^2 - c'_{11}R'M') \end{aligned}$$

$$\begin{aligned} H = [&AC\varepsilon^2 bR'M' + iDACc_{44}R'M' + A\varepsilon^2 b(ch\Omega')^2 R'M' + iDA(ch\Omega')^2 Cc_{44}R'M' - AQ'^2\varepsilon^4 b - \\ &iDAQ'^2\varepsilon^2 c_{44}M' / h + (ch\Omega')^2 C\varepsilon^2 bR'M' + iD(ch\Omega')^2 Cc_{44}R'M' + (ch\Omega')^4\varepsilon^2 bR'M' \\ &+ iD(ch\Omega')^4 c_{44}R'M' - (ch\Omega')^2 Q'^2\varepsilon^4 b - iD(ch\Omega')^2 Q'^2\varepsilon^2 c_{44}M' / h - 2Bc^2h^3\Omega'\varepsilon^2 bR'M' - \\ &2iDBc^2h^3\Omega'c_{44}R'M' - 4\Omega'^2c^4h^4\varepsilon^2 bR'M' + 4D\Omega'^2c^4h^4c_{44}R'M' + 2\Omega'c^2h^3Q'M' + \\ &2iD\Omega'c^2h^3\varepsilon Q'c_{44}M'^2 / h] / (M'^2 - c'_{11}R'M') \end{aligned} \tag{11}$$

Using Eq. (10), the proposed solutions of equation(5) can be written as

$$\varphi = \sum_{i=1}^{3}[A_i J_n(\alpha_i x) + B_i Y_n(\alpha_i x)]\cos n\theta$$

$$w = \sum_{i=1}^{3} d_i[A_i J_n(\alpha_i x) + B_i Y_n(\alpha_i x)]\cos n\theta$$

$$\xi = \sum_{i=1}^{3} e_i [A_i J_n(\alpha_i x) + B_i Y_n(\alpha_i x)] \cos n\theta \tag{12}$$

Where, α_i^2 are the non-zero roots of the equation

$$\alpha^6 - S\alpha^4 + U\alpha^2 - H = 0 \tag{13}$$

Where, d_i and e_i are given by

$$(1 + c'_{13})\varepsilon d_i + M' e_i = (c'_{11}\alpha_i^2 - (ch)^2 - \varepsilon^2)$$

$$(-\alpha_i^2 + (ch)^2 - c'_{33}\varepsilon^2)d_i - Q'\varepsilon e_i = (1 + c'_{13})\varepsilon\alpha_i^2 \tag{14}$$

Solving equation (7a) we have

$$\psi = [A_4 J_n(\alpha_4 x) + B_4 Y_n(\alpha_4 x)] \sin n\theta \tag{15}$$

Where

$$\alpha_4^2 = \frac{(ch)^2 - \varepsilon^2}{c'_{66}} \tag{16}$$

Frequency equation

For traction-free boundary conditions in the present study, stresses must vanish on the inner and outer surfaces of the hollow cylinder, i.e.,

$$\sigma = \sigma_{rr} = \sigma_{r\theta} = \sigma_{rz} = 0 \text{ at } r = a',\ \ b' \tag{17}$$

where $a' = \frac{a}{h}$ and $b' = \frac{b}{h}$

Using equations (5),(12),(15) in (1), we obtain frequency equation in the form

$$\left|a_{ij}\right| = 0 \ \ \text{(i,j=1,2,….,8)} \tag{18}$$

The expressions of a_{ij} coefficients are given in Appendix A. (18)

Numerical results and discussion

We calculated the numerical findings of the frequency equation considering the Matlab package for the hydrated bone. The frequency equation has an infinite number of roots because it is transcendental. The frequencies (i.e., the roots of Eq. (20)), $n = 0$, the axisymmetric mode, and flexural $n = 1, 2$ modes are provided. The results are assessed in the range $0 < \varepsilon_1 < 4$ and $0 < ch < 4$, with the ratio of $\frac{b}{a} = 3.0$. The values of the elastic constant of the bone are derived from [8], and the poroelastic constant is assessed using the expression given by

$$Q = \frac{f\left(1 - f - \frac{\delta}{\chi}\right)}{\left(\gamma + \delta + \frac{\delta^2}{\chi}\right)}, \qquad R = \frac{f^2}{\left(\gamma + \delta + \frac{\delta^2}{\chi}\right)}. \tag{19}$$

The expressions of γ, δ, χ are given by

$$\chi = \frac{3(1-2\nu)}{E}, \quad \delta = 0.6\chi \quad and \;\; \gamma = f(c-\delta) \tag{20}$$

where, c equals zero for the incompressibility of the fluid.

The porosity of the bones of the people aged 35-40 years equals 0.24. To assess one more poroelastic constant, $\frac{M}{Q} \cong \frac{c_{12}}{c_{13}}$ as the value M is not provided. Because the fluid is isotropic, $b_{rr} = b_{zz}$. The density of the fluid in the porospace, the permeability of the medium, and mass density of the bone can be assessed. For different frequency values, the wave numbers, the wave velocity, and the attenuation coefficients are derived from the frequency equation (Table 1).

C_{11}	C_{12}	C_{13}	C_{33}	C_{44}	a	b
2.12	0.95	1.02	3.76	0.75	0.8	1.4

Table 1: The main geometric dimension of the femur and the corresponding material properties

Figure 1: shows that the schematic of the problem.

Figure 2: shows that the variation of thesecular determinant $|a_{ij}|$, wave velocity $\mathrm{Re}(|a_{ij}|)$ and attenuation coefficient $\mathrm{Im}(|a_{ij}|)$ with respect to thickness h for different values of wave number k. It is observed that the,secular determinant, wave velocity and attenuation coefficient increase with increases of the wave number, while it increases with increasing of the thickness in the interval $0 \le h \le 0.08$, as well as there is no significant variation on the secular determinant, wave velocity and attenuation coefficient in the interval $0.08 \le h \le 1$.

Figure 3: shows that the variation of the secular determinant $|a_{ij}|$, wave velocity $\mathrm{Re}(|a_{ij}|)$ and attenuation coefficient $\mathrm{Im}(|a_{ij}|)$ with respect to thickness h for different values of porosity f. It is obvious that the secular determinant, wave velocity and attenuation coefficient increase with increases of the porosity, while it increases with increasing of the thickness in the interval $0 \le h \le 0.08$, as well, there is no significant variation on the secular determinant,wave velocity and attenuation coefficient in the interval $0.08 \le h \le 1$.

Figure 4: shows that the variation of the secular determinant $|a_{ij}|$, wave velocity $\mathrm{Re}(|a_{ij}|)$ and attenuation coefficient $\mathrm{Im}(|a_{ij}|)$ with respect to thickness for different values of rotation while the attenuation coefficient increases with increasing of rotation. It is observed that the secular determinant and wave velocity increase with increases of the rotation, while it increases with increasing of the thickness in the interval $0 \le h \le 0.08$, as well, there is no significant variation on the secular determinant, wave velocity and attenuation coefficient in the interval $0.08 \le h \le 1$. This behavior was projected by other models [28,29] and experimental studies [30,31].

The case of the complex conjugate roots has not been handled. These cases possibly happen for specific combinations of bone property values. Consequently, much more complex computation is required since for each step both the real and imaginary parts of the determinant components must be calculated. We handled those cases successfully (Figures 2,3 and 4).

(a) **(b)**

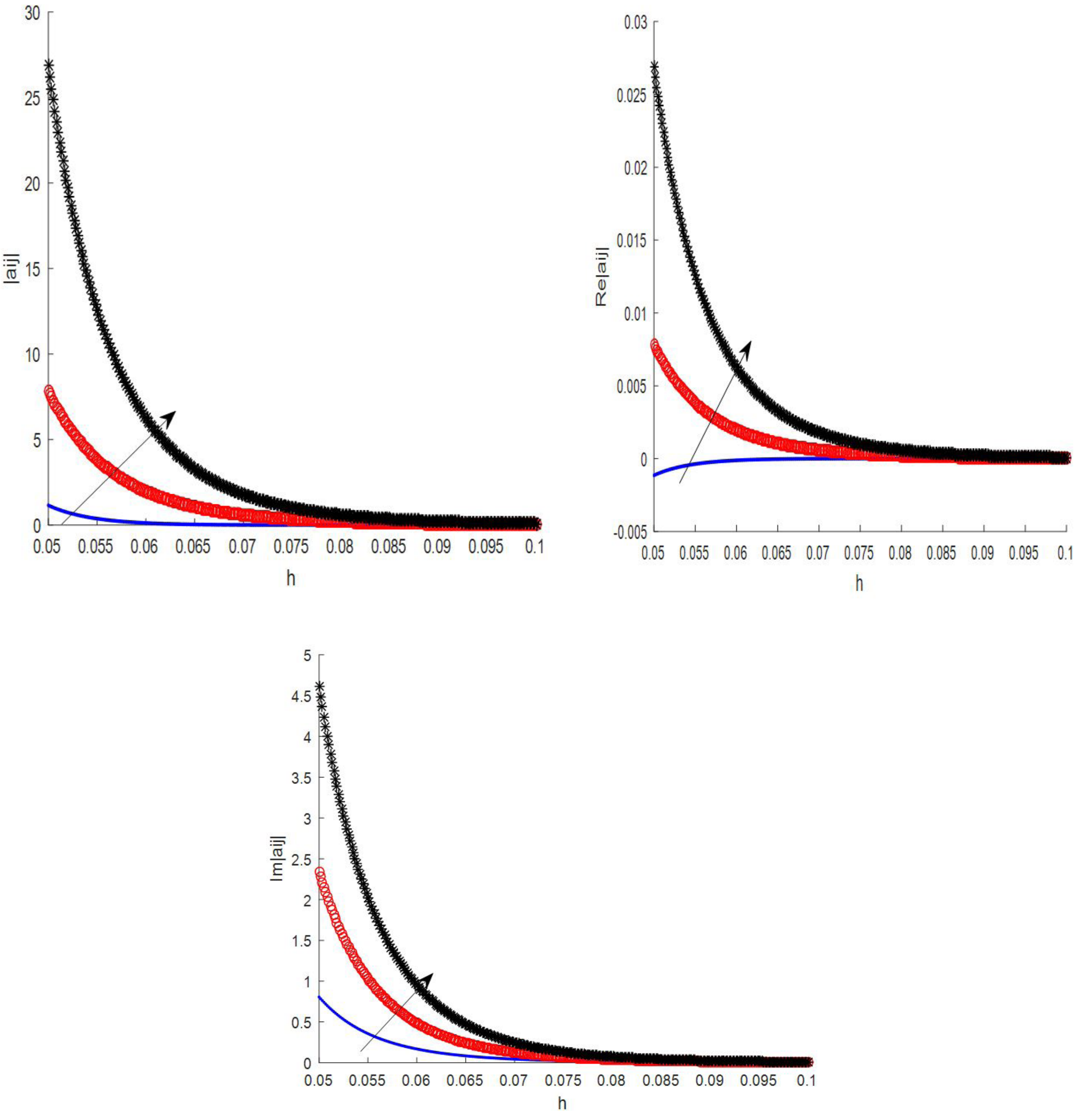

(c)

Figure 2: Variations of the secular determinant $|a_{ij}|$, wave velocity $\mathrm{Re}(|a_{ij}|)$ and attenuation coefficient $\mathrm{Im}(|a_{ij}|)$ with respect to the thickness h for different values of wave number … k=0.5, ooo k=1, *** k=1.5.

(a) **(b)**

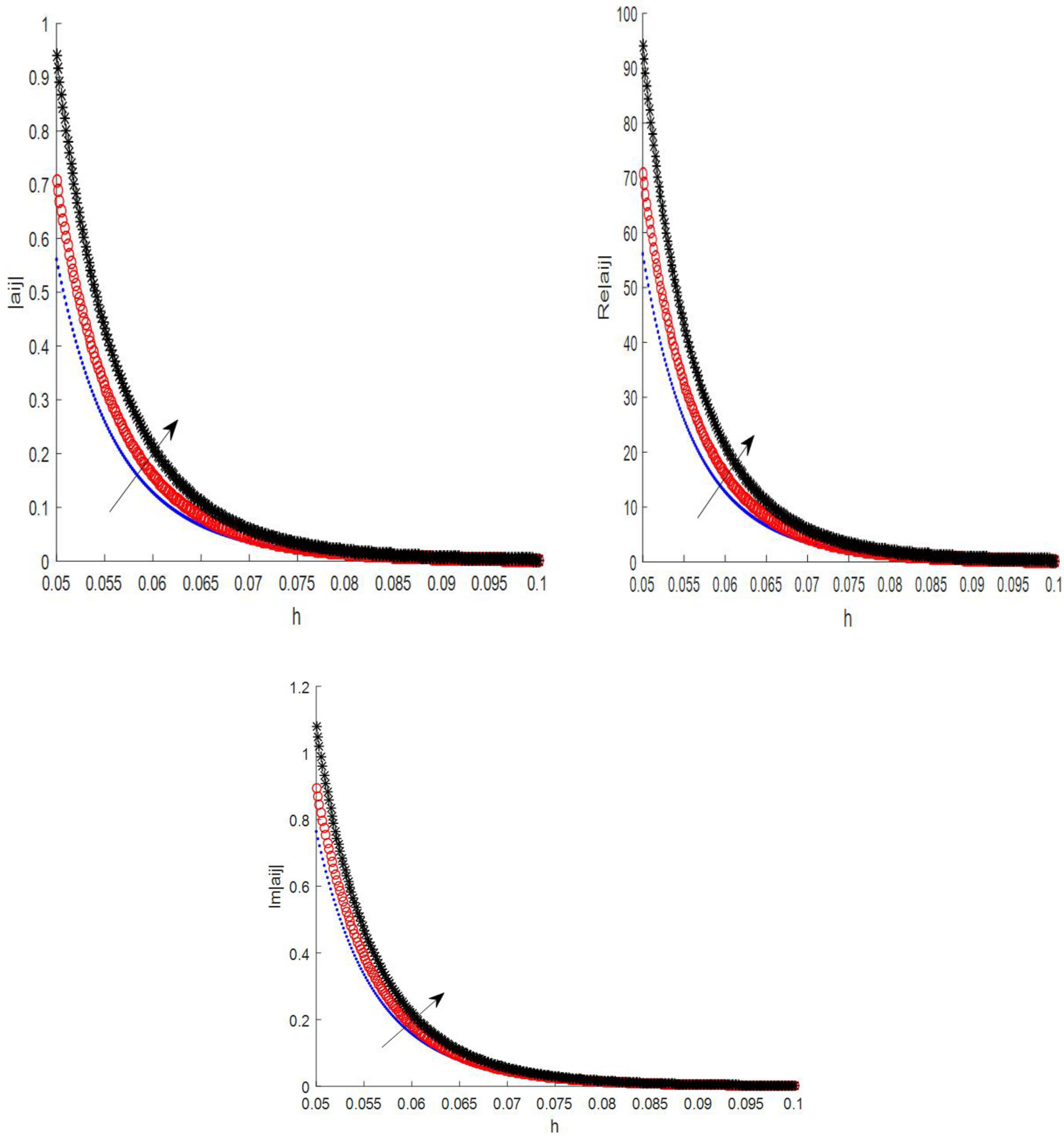

(c)

Figure 3: Variations of the secular determinant $|a_{ij}|$, wave velocity $\mathrm{Re}(|a_{ij}|)$ and attenuation coefficient $\mathrm{Im}(|a_{ij}|)$ with respect to the thickness h for different values of porosity ... $f = 0.24$, ooo $f = 0.26$, *** $f = 0.28$.

(a) (b)

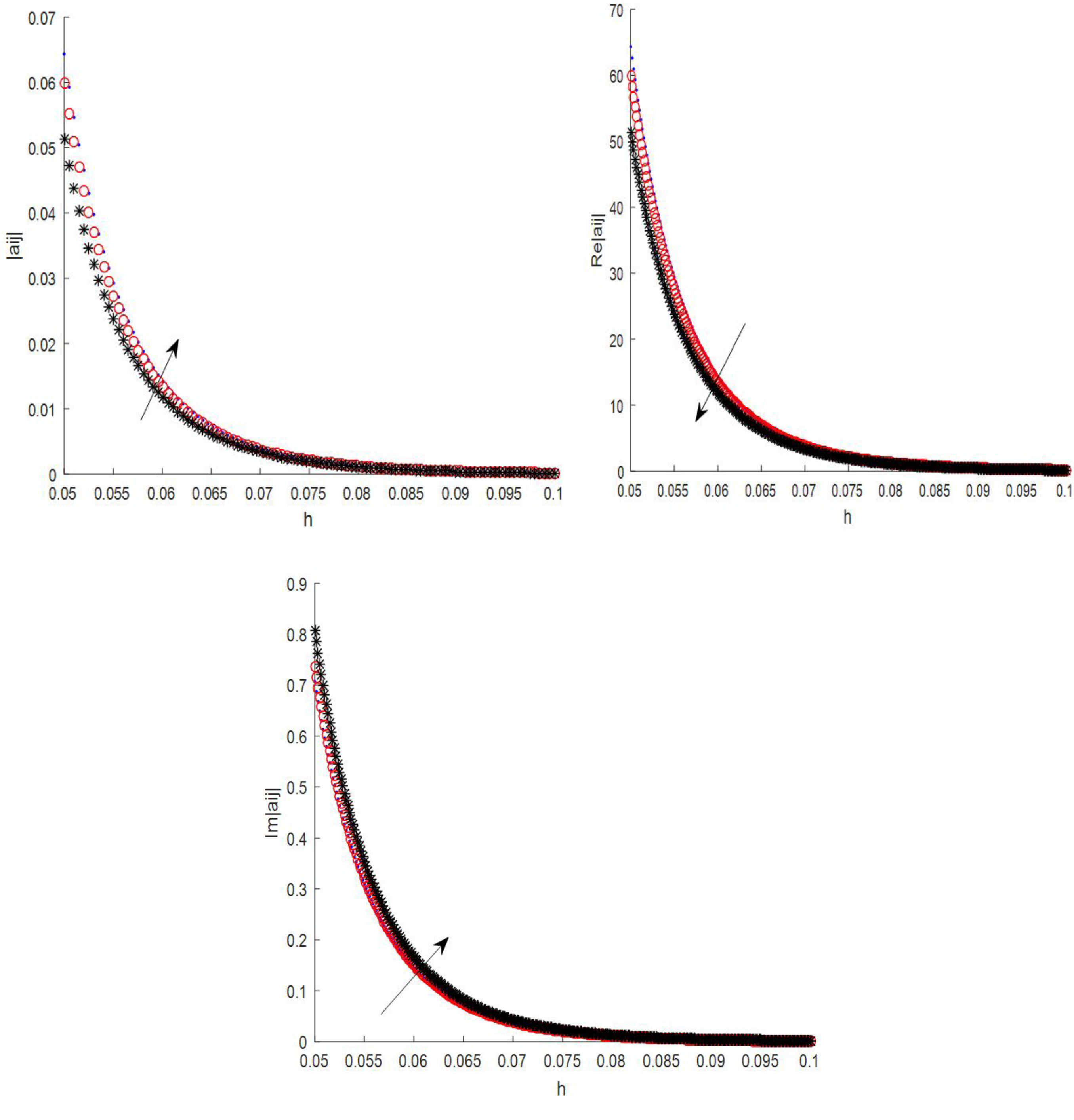

(c)

Figure 4: Variations of the secular determinant $\left|a_{ij}\right|$, wave velocity $\mathrm{Re}(\left|a_{ij}\right|)$ and attenuation coefficient $\mathrm{Im}(\left|a_{ij}\right|)$ with respect to the thickness h for different values of … Ω =2, ooo Ω =4, *** Ω=6.

Conclusion

After examining the propagation of waves in hollow poroelastic bone with a circular cylindrical cavity of infinite extent, the authors conclude that

1. Bones are heterogeneous and anisotropic. The solid part is perfectly elastic and the fluid part is Newtonian viscous and compressible. The pores are interrelated and the flow of fluid resulting from bone deformation is controlled by Darcy's law.

2. We explored the propagation of waves in an infinite hollow rotating cylinder of crystal class 6. We did the analysis, and the solution to the problem was described concerning the potential function. The resulting frequency equation was solved numerically.

3. The numerical results illustrated that, except for the mechanical conditions, the rotation, wave number and the porosity can influence the propagation of waves on the bone. This feature can be taken into account and employed in controlling the healing process of the injured bones. All results are obtained based on the numerical model that may differ from those of the individual bone materials. Thus, more experimental validation is essential before using the present results for the clinical practice.

4. We made observations of the effect of the rotation, wave number and porosity in wave propagation in wet bone's surface.

5. In short, we can have a theoretical simulation of the in vivo case by taking thme properties of the muscle and the skin that cover bones in the limbs.

Appendix

References

1. Gurijala R, Perati MR (2020) Study of radial vibrations in thick walled hollow dissipative poroelastic spherical shell on elastic foundation. Material Physics and Mechanics 44: 422.

2. Abd-Alla AM, Abo-Dahab SM (2013) Effect of magnetic field on poroelastic bone model for internal remodeling, Applied Mathematics and Mechchanics 34: 889-906.

3. Fotiadis DI, Foutsitzi G, Massalas CV (1999) Wave propagation modeling in human long bones. Acta Mechanica 137: 65-81.

4. Papathanasopoulou VA, Fotiadis DI, Massalas CV (2004) A theortical analysis of surface remodeling in long bones, International Journal of Engineering Science 42: 395-409.

5. Biot MA (1956) Theory of propagation of elastic waves in a fluid-saturated porous solid. I: low-frequency range, Journal of the Acoustical Society of America 28: 168-78.

6. Fotiadis DI, Foutsitzi G, Massalas CV (1999) Wave propagation modeling in human long bones. Acta Mechanica 137: 65-81.

7. Boyle C, Kim IY (2011) Three-dimensional micro-level computational study of Wolff's law via trabecular bone remodeling in the human proximal femur using design space topology optimization, Journal of Biomechanics 44: 935-42.

8. Mengoni M, Ponthot JP (2010) Isotropic continuum damage/repair model for alveolar bone remodeling,Journal of Computational and Applied Mathematics 234: 2036-45.

9. Papathanasopoulou VA, Fotiadis DI, Foutsitzi G, Massalas CV (2002) A poroelastic bone model for internal remodeling, International Journal of Engineering Science 40: 511-30.

10. Qu C, Qin QH, Kang Y (2006) A hypothetical mechanism of bone remodeling and modeling under electromagnetic loads. Biomaterials 27: 4050-7.

11. Hazelwood SJ, Martin RB, Rashid MM, Rodrigo JJ (2001) A mechanistic model for internal bone remodeling exhibits different dynamic responses in disuse and overload. Journal of Biomechanics 34: 299-308.

12. Vahdati A, Rouhi G (2009) A model for mechanical adaptation of trabecular bone incorporating cellular accommodation and effects of microdamage and disuse. Mechanics, Research Communications 36: 284-93.

13. Malachanne E, Dureisseix D, Jourdan F (2011) Numerical model of bone remodeling sensitive to loading frequency through a poroelastic behavior and internal fluid movements. Journal of the Mechanical Behavior of Biomedical Material 4: 849-57.

14. Zumsande M, Stiefs D, Siegmund S, Gross T (2011) General analysis of mathematical models for bone remodeling. Bone 48: 910-7.

15. Ramtani S, He QC (2014) Internal bone remodeling induced by metallic pin fitted into medulla of a long bone having cylindrical anisotropy: Theoretical predictions. International Journal of Engineering Science 82: 124-39.

16. Ganghoffer JF (2012) A contribution to the mechanics and thermodynamics of surface growth. Application to bone external remodeling, International Journal of Engineering Science 50: 166-91.

17. Cowin SC, Firoozbakhsh K (1981) Bone remodeling of diaphysial surfaces under constant load: Theoretical predictions, Journal of Biomechanics 14: 471-84.

18. Tsili MC (2000) Theoretical solutions for internal bone remodeling of diaphyseal shafts using adaptive elasticity theory. Journal of Biomechanics 33: 235-9.

19. Jang IG, Kim IY (2010) Computational simulation of simultaneous cortical and trabecular bone change in human proximal femur during bone remodeling. Journal of Biomechanics 43: 294-301.

20. Martínez GJ, Aznar MG, Doblaré M, Cerrolaza M (2006) External bone remodeling through boundary elements and damage mechanics. Mathematics and Computers in Simulation 73: 183-99.

21. Qin QH, Qu C, Ye J (2005) Thermoelectroelastic solutions for surface bone remodeling under axial and transverse loads. Biomaterials 26: 6798-810.

22. Kameo Y, Adachi T, Hojo M (2011) Effects of loading frequency on the functional adaptation of trabeculae predicted by bone remodeling simulation. Journal of the Mechanical Behavior of Biomedical Materials 4: 900-8.

23. González Y, Cerrolaza M, González C (2009) Poroelastic analysis of bone tissue differentiation by using the boundary element method, Engineering Analysis with Boundary Elements 33: 731-40.

24. Qin QH, Qu C, Ye J (2005) Thermoelectroelastic solutions for surface bone remodeling under axial and transverse loads. Biomaterials 26: 6798-810.

25. Abd-Alla AM, Abo-Dahab SM (2013) Effect of magnetic field on poroelastic bone model for internal remodeling. Applied Mathematics and Mechanics 34: 889-906.

26. Knahr K, Karamat L (2006) Influence of enhanced proximal press-fit on bone remodelling after implantation of a cementless tapered stem. Journal of Biomechanics 39: S14.

27. Kumar NC, Dantzig JA, Jasiuk IM, Robling AG, Turner CH (2010) Numerical modeling of long bone adaptation due to mechanical loading: correlation with experiments. Annals of Biomedical Engineering 38: 594-604.

28. Grillo A, Prohl R, Wittum G (2016) A poroplastic model of structural reorganisation in porous media of biomechanical interest. Continuum Mechanics and Thermodynamics 28: 579-601.

29. Abd-Alla AM, Abo-Dahab SM, Ateeq R, Khder MA (2020) Effect of rotation on wave propagation through a poroelastic wet bone with cavity. Multidiscipline Modeling in Materials and Structures 16: 53-72.

30. Woo SLY, Kuri SC, Dillon WA, Amiet D, White FC, Akenson WH (1981) The effect of prolonged physical training on the properties of long bone – a study of Wolff's law. J Bone Int Surg 36-A: 780-7.

31. Cowin SC, Hart RT, Balser JR, Kohtn DH (1981) Functional adaptation in long bone. Established in vivo values for surface remodling rate coefficient. J Biomech 18: 471-84.

32. Abd-Alla AM, Abo-Dahab SM, Mahmoud SR (2011) Wave propagation modeling in cylindrical human long wet bones with cavity. Meccanica 46: 1413-28.